

Infinite joint species distribution models

Federica Stolf¹ and David B. Dunson²

¹Department of Statistical Sciences, University of Padova, Italy

²Department of Statistical Science, Duke University, Durham, NC, USA

Abstract

Joint species distribution models are popular in ecology for modeling covariate effects on species occurrence, while characterizing cross-species dependence. Data consist of multivariate binary indicators of the occurrences of different species in each sample, along with sample-specific covariates. A key problem is that current models implicitly assume that the list of species under consideration is predefined and finite, while for highly diverse groups of organisms, it is impossible to anticipate which species will be observed in a study and discovery of unknown species is common. This article proposes a new modeling paradigm for statistical ecology, which generalizes traditional multivariate probit models to accommodate large numbers of rare species and new species discovery. We discuss theoretical properties of the proposed modeling paradigm and implement efficient algorithms for posterior computation. Simulation studies and applications to fungal biodiversity data provide compelling support for the new modeling class.

Keywords: Bayesian; Ecology; Indian buffet process; Multivariate binary response; Multivariate probit model.

1 INTRODUCTION

Joint species distribution models are routinely used in ecology. The focus is on modeling covariate effects and cross-species dependence in occurrence. Current models implicitly assume that a list of the p species under study can be pre-specified. Letting $j \in \{1, \dots, p\}$ index the species in this list, species co-occurrence data consist of an $n \times p$ matrix Y of binary indicators with $y_{ij} = 1$ if species j was found in sample i and $y_{ij} = 0$ otherwise. Joint species distribution models define a multivariate binary regression for $y_i = (y_{i1}, \dots, y_{ip})^\top$ given covariates $x_i = (x_{i1}, \dots, x_{iq})^\top$. For example, the popular `HMSC` package relies on a Bayesian probit latent factor model (Ovaskainen et al., 2016; Tikhonov et al., 2020).

For common species the above framework is highly successful, providing key insights into the role of biotic and abiotic factors on community assembly. However, with the emergence of automated

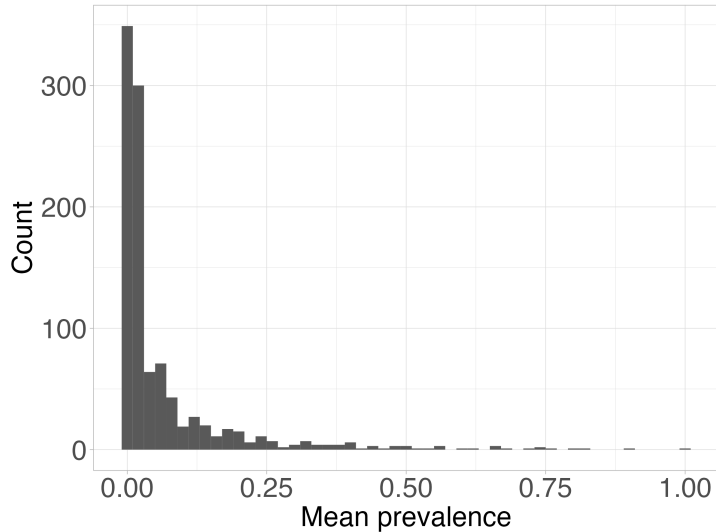


Figure 1: Empirical species occurrence probabilities for fungi data in a Finnish study.

biodiversity monitoring methods for highly diverse groups of organisms, such as arthropods and fungi, critical problems emerge. Firstly, while biomass is dominated by a relatively small number of common species, the vast majority of species on Earth are extremely rare. Hence, it is impossible to prespecify a list of species under study in advance of collecting data. In a given study, we tend to observe a minute fraction of the species known to occupy the study region. In addition, it is common to discover species unknown to science. Given these problems, current practice chooses the list of species to be considered in the joint species analysis in a post-hoc manner, typically discarding the rare species making up most of the biodiversity.

To make this motivation concrete, in Figure 1 we plot empirical fungi species occurrence probabilities from Abrego et al. (2018). Although we use the word species for simplicity, ecologists instead refer to operational taxonomic units (OTU). The OTUs are obtained by applying DNA barcoding to fungal samples, and then implementing a taxonomic classifier (Somervuo et al., 2016). Similar data on fungi co-occurrence were the focus of a recent *Nature* paper (Abrego et al., 2024); the authors analyzed the data using the HMSC package but focusing on the few 100 most common species and discarding $\sim 20,000$ rare species. However, rare species have a critical impact on biodiversity, so ignoring them limits the conclusions that can be drawn from the analysis.

To motivate directions forward in addressing these problems, consider the multivariate probit model (Chib and Greenberg, 1998):

$$\begin{aligned}
 y_{ij} &= \mathbb{1}(z_{ij} > 0), & z_i &= (z_{i1}, \dots, z_{ip})^\top \\
 z_i &= B^\top x_i + \varepsilon_i, & \varepsilon_i &\sim N_p(0, \Sigma),
 \end{aligned} \tag{1}$$

with $B = (\beta_1, \dots, \beta_p)$ a $q \times p$ matrix of regression coefficients, Σ a correlation matrix and $\mathbb{1}(\cdot)$ the indicator function. Under this model, the marginal probability of occurrence of species j conditionally on covariates $x_i = x$ is $\pi_j = \Phi(x^\top \beta_j)$, with $\Phi(\cdot)$ the standard normal cumulative distribution function. Dependence in co-occurrence between species j and j' is captured by $\text{cor}(z_{ij}, z_{ij'}) = \sigma_{jj'}$, the j, j' element of matrix Σ .

In implementing Bayesian analyses of fungi biodiversity data using model (1), there are fundamental problems. The foremost is, as described above, we cannot tie down the identities of the different binary outcomes (species) $j = 1, \dots, p$ in advance. Indeed, we expect to regularly discover new species as we collect additional samples, so that the total numbers of species in n samples may be substantially less than that in $n + m$ samples. Hence, we need a mechanism to allow a growing number of binary outcomes.

A related problem is considered in the literature on infinite latent feature models and the Indian Buffet Process (IBP) (Griffiths and Ghahramani, 2011). The IBP is a distribution on binary matrices with a finite number of rows and an unbounded number of columns, where rows are exchangeable and columns are independent. The IBP allows new binary features (species) to be discovered as new samples are collected, but does not characterize within-sample dependence in species occurrences. Potentially, we could use model (1) setting p to a large number with a buffer incorporated to allow new species to be added as the sample size increases. However, simply adding a buffer without careful consideration is ad hoc and may have unanticipated negative consequences, as we will show later in the manuscript.

Motivated by the above considerations, the focus of this article is on developing a general new infinite joint species distribution modeling framework borrowing key ideas from the literature on infinite latent feature models to appropriately extend multivariate probit-style hierarchical regression models. The proposed framework avoids discarding rare species in inferring covariate effects on species communities and in investigating cross-species dependence. In addition, a key advantage over traditional fixed species list models, is that our framework enables prediction of the number of additional species that would be discovered if m additional samples were collected after an initial n samples. Such predictions are of substantial interest in making decisions about whether to collect additional data in a biodiversity monitoring study.

Our framework adds to the ongoing literature on generalizations of the classical IBP model to allow additional flexibility; refer, for example, to Broderick et al. (2013); Gershman et al. (2014); Di Benedetto et al. (2020); Camerlenghi et al. (2024); Williamson et al. (2010); Warr et al. (2022). In this regard, we are the first to incorporate dependence within samples in feature occurrence. Although our focus is on biodiversity applications, our methods have direct applications in other areas ranging from microbiome data (Zhao et al., 2021) to studies of genetics variants (Lee et al., 2010).

2 PROPOSED MODELING FRAMEWORK

2.1 MODEL SPECIFICATION

We introduce a novel tracking rare and abundant co-occurrences in ecology (**TRACE**) modeling framework. Let Y be a binary matrix of species occurrences with n rows and an unbounded number of columns, where $y_{ij} = 1$ indicates species j was found in sample i . The matrix Y is sampled as a sequential process to accommodate a growing number of species. In this way, we avoid fixing species identities in advance, but let the model adapt to the growing complexity of the data as new species are discovered. As commonly done in infinite latent feature models, we derive a distribution on infinite binary matrices by starting with a truncation level p for the number of species and then taking the limit as $p \rightarrow \infty$.

Our proposed infinite joint species distribution model is defined through a latent Gaussian construction. Let $z_i = (z_{i1}, \dots, z_{ip})^\top \in \mathbb{R}^p$ denote a p -variate latent continuous variable for $i = 1, \dots, n$ and let y_{ij} be 1 or 0 according to the sign of z_{ij} . Let $x_i = (x_{i1}, \dots, x_{iq})^\top$ be the covariate for each sample i and $\beta_j = (\beta_{j1}, \dots, \beta_{jq})^\top$ the regression coefficients specific to species j , with q the number of covariates. The **TRACE** modelling framework is defined as

$$\begin{aligned} y_{ij} &= \mathbf{1}(z_{ij} > 0), & z_{ij} &= \alpha_j + x_i^\top \beta_j + \varepsilon_{ij}, \\ \alpha_j &\sim N(\mu_p, \tau_p), & \varepsilon_i &\sim N_p(0, \Sigma), \end{aligned} \tag{2}$$

where $\alpha = (\alpha_1, \dots, \alpha_p)^\top$ is a p -dimensional vector of random intercepts, with α_j controlling the baseline commonness of species j , and $\Sigma = \{\sigma_{jj'}\}$ is a $p \times p$ positive definite correlation matrix, with $\sigma_{jj'}$ controlling dependence in occurrence of species j and j' . We will later describe hierarchical models for $B = (\beta_1, \dots, \beta_p)$ and Σ to enable borrowing of information.

The hierarchical structure on the intercepts α_j plays a critical role in the model specification. In order to accurately characterize the data, we need to allow there to be a small proportion of common species and a large number of very rare species. In addition, in the limit as $p \rightarrow \infty$, the number of species observed in a sample $\sum_{j=1}^p y_{ij}$ should be almost surely finite. The hyperparameters μ_p and τ_p in the prior for α_j play a crucial role in determining the induced likelihood of z_i and thus also the likelihood of Y . These hyperparameters control the distribution of the number of species within each sample, as well as the rate of growth in the total number of species, corresponding to the number of non-zero columns of Y as n increases.

We will show in the next section that the default values

$$\mu_p = (1 + \tau_p^2)^{1/2} \Phi^{-1} \left(\frac{\gamma}{\gamma + p} \right), \quad \tau_p = (2 \log p)^{1/2}, \quad \gamma \in \mathbb{R}^+ \tag{3}$$

lead to several desirable properties as p grows. Also, in the baseline case in which there are no covariates and $\Sigma = I$, **TRACE** is shown to have similar behavior to the popular Indian buffet process. Hence, **TRACE** can be viewed as providing a useful framework for extending the **IBP** to incorporate within-sample and covariate dependence in feature occurrences.

The **TRACE** framework corresponds to a probit-Bernoulli process: it generates species from a Bernoulli process with probabilities drawn from an underlying probit process. Hence, marginally for each of the species we have $\text{pr}(y_{ij} = 1 \mid \beta_j, \alpha_j, x_i) = \Phi(\alpha_j + x_i^\top \beta_j)$. For rare species, there is insufficient information in the data to accurately estimate the species-specific regression coefficients. To address this problem, it is natural to choose a hierarchical structure to borrow information across the different species. Hence, we let

$$\beta_j \mid \nu, \Psi \sim N_q(\nu, \Psi), \quad (\nu, \Psi) \sim \text{NIW}(\nu_0, \iota, d, \Xi), \quad (4)$$

where $\text{NIW}(\nu_0, \iota, d, \Xi)$ is a Normal-Inverse Wishart prior distribution.

Similarly to the usual multivariate probit model (1), the likelihood of Y under the **TRACE** model cannot be expressed in a closed form, as it requires integrating over a multivariate normal distribution. However, there is a rich literature on efficient posterior computation algorithms for (1), which we will leverage. We demonstrate several compelling theoretical properties that provide strong support for **TRACE**. For example, we will show that the limiting number of non-zero entries in Y as $p \rightarrow \infty$ is almost surely finite. This ensures that the number of sampled species will be finite even in the limiting case.

2.2 PROPERTIES AND CONNECTION TO INDIAN BUFFET PROCESSES

In this section we present some theoretical properties motivating the modeling framework described in (2) and (3). Proofs are given in the supplementary materials. We also highlight relationships with the Indian buffet process. To emphasize this connection, we start by considering the **TRACE** model without covariates:

$$y_{ij} = \mathbb{1}(z_{ij} > 0), \quad z_{ij} = \alpha_j + \varepsilon_{ij}, \quad \alpha_j \sim N(\mu_p, \tau_p), \quad \varepsilon_i \sim N_p(0, \Sigma) \quad (5)$$

with the values for μ_p and τ_p in equation (3). We recall that the Indian buffet process is induced through a Beta-Bernoulli process: $y_{ij} \mid \pi_j \sim \text{Bernoulli}(\pi_j)$, $\pi_j \sim \text{Beta}(\gamma/p, 1)$, where the π_j s and y_{ij} s are all mutually independent (Thibaux and Jordan, 2007).

First, we prove that in the limiting case as $p \rightarrow \infty$, the expected number of non-zero entries is finite. More specifically, Theorem 1 shows that the no covariates **TRACE** model has the same number of expected features as the **IBP**, yielding an intuitive interpretation for the parameter γ . It also shows that in the simple case with $\Sigma = I$, where there is no dependence among species as in the **IBP**, the

number of species per sample has the same distribution as the IBP.

Theorem 1. *Consider the no covariates TRACE model and let $n_i = \sum_{j=1}^p y_{ij}$. Then $\lim_{p \rightarrow \infty} E(n_i) = \gamma$, for each $i = 1, \dots, n$. If we further assume $\Sigma = I$, then $n_i \sim Po(\gamma)$ for $p \rightarrow \infty$.*

Theorem 1 ensures that the number of sampled species is finite, so that $\text{pr}(n_i < \infty) = 1$. In the following proposition, we characterize the limiting variance of n_i in the no covariates TRACE model with $\Sigma \neq I$. In the $\Sigma = I$ case, the limiting variance is γ due to the $n_i \sim Po(\gamma)$ property.

Proposition 1. *Consider the no covariates TRACE model and assume that $\sigma_{jj'} \in \{\rho_1, \dots, \rho_k\}$ with $k \in \mathbb{N}$. Then $\gamma + \gamma^2/2 \{\min_k |\exp(\rho_k) - 1|\} \leq \lim_{p \rightarrow \infty} \text{var}(n_i) \leq \gamma + \gamma^2/2 \{\max_k |\exp(\rho_k) - 1|\}$, for each $i = 1, \dots, n$.*

Proposition 1 provides bounds for the limiting variance of n_i . For tractability in deriving and interpreting the bounds, we make the simplifying assumption that the between-species correlations belong to a finite set of possible values. If some pairs of species are uncorrelated, the lower bound is γ while if some pairs of species are perfectly correlated the upper bound is $\gamma + \gamma^2\{\exp(1) - 1\}/2$. These extreme case bounds can be shown to hold even when the finite set assumption is violated. The above results are extended to the general TRACE model, which allows inclusion of covariates, in Theorem 2.

Theorem 2. *Consider the TRACE model and let $g_i = \exp\{x_i^\top \nu + (1/2)x_i^\top \Psi x_i\}$. Then for $i = 1, \dots, n$, (i) $\lim_{p \rightarrow \infty} E(n_i) = \gamma g_i$; (ii) if we further assume $\sigma_{jj'} \in \{\rho_1, \dots, \rho_k\}$ with $k \in \mathbb{N}$, we have $\gamma g_i(1 + \gamma g_i/2) \{\min_k |\exp(\rho_k) - 1|\} \leq \lim_{p \rightarrow \infty} \text{var}(n_i) \leq \gamma g_i(1 + \gamma g_i/2) \{\max_k |\exp(\rho_k) - 1|\}$.*

The above theorem provides valuable insights into the impact of covariates on biodiversity measured in terms of sample-specific species richness, that is the number of species per sample. The expected sample-specific species richness is simply γg_i , where $\log(g_i)$ follows a quadratic regression in covariates x_i with the linear coefficients corresponding to the mean $\nu = E(\beta_j)$ and the quadratic coefficients to the covariance $\Psi = \text{cov}(\beta_j)$ of the population-distribution of species-specific coefficients in (4). Obtaining such a simple induced model characterizing the impact of covariates on biodiversity is a major advantage of TRACE. For example, one can directly assess the impact of climate or environmental disruption covariates on sample-specific species richness using Theorem 2.

A critical property of real world biodiversity data is that we expect a small number of common species having π_j values not close to zero with the remaining having $\pi_j \approx 0$. This leads to considerable sparsity in the Y data matrix with many columns having few 1s. The following proposition supports sparsity of the TRACE model.

Proposition 2. *The data matrix Y sampled under the TRACE model is sparse in the sense that $\lim_{p \rightarrow \infty} \text{pr}(y_{ij} = 1) = \lim_{p \rightarrow \infty} (\gamma/p)/(\gamma/p + 1) = 0$ holds for each $i = 1, \dots, n$.*

Proposition 2 shows that the marginal probabilities go to zero at a linear rate as p grows; this same sparsity property holds for the IBP.

In addition to sparsity of Y , a key aspect of the data is that some of the species are common. Such species have π_j values in the right tail of the population distribution of the π_j s across j . In order for the model to be realistic in the motivating biodiversity contexts, we need the sparsity property of Proposition 2 to not rule out the presence of common species. Thus, the focus is studying the right tail of the distribution of π_j s across the species. In definition 1 we provide a formal notion of common species.

Definition 1. Let Y be an $n \times p$ binary matrix of species occurrence indicators and let $\pi_j = \text{pr}(y_{ij} = 1)$ for $i = 1, \dots, n$. Species j is common if $\text{pr}(\pi_j > \epsilon)$ for fixed threshold $\epsilon > 0$.

Let $c_j^{(\epsilon)} = \mathbb{1}(\pi_j > \epsilon)$ indicate whether the j th species is common, for $j = 1, \dots, p$, and $c^{(\epsilon)} = \sum_{j=1}^p c_j^{(\epsilon)}$ denote the number of common species for threshold ϵ . The latter quantity summarizes the behaviour of the distribution of the marginal probabilities across j and characterizes the right tail of this distribution for high values of ϵ .

For the IBP model, the expected number of common species is

$$E(c^{(\epsilon)}) = \lim_{p \rightarrow \infty} \sum_{j=1}^p \text{pr}(\pi_j > \epsilon) = \lim_{p \rightarrow \infty} p\{1 - B_\epsilon(\gamma/p, 1)\} = \lim_{p \rightarrow \infty} p(1 - \epsilon^{\gamma/p}) = -\gamma \log \epsilon,$$

where $B_x(a, b)$ is the regularized incomplete beta function. This is a novel result to our knowledge. The following proposition states a related result for the no covariates TRACE model.

Proposition 3. For no covariates TRACE model the expected number of common species is $\lim_{p \rightarrow \infty} E(c^{(\epsilon)}) = \gamma \exp\{-\Phi^{-1}(\epsilon) - 0.5\}$.

Hence, the expected number of common species under TRACE differs somewhat from that for the IBP. However, the functional relationship with the commonness threshold ϵ is similar, as illustrated in Figure 2. This figure also compares the expected number of common species under the TRACE and IBP models with the empirical values observed in our motivating data. For this plot we utilized an optimized value of γ , set to 70. Notably, the theoretical curves for the TRACE and IBP models align closely, indicating that both models exhibit comparable behavior. Moreover, they effectively capture the observed total number of common species in the fungi co-occurrence data. The following proposition adapts the result to the general TRACE framework.

Proposition 4. Let $c_{ij}^{(\epsilon)} = \mathbb{1}\{\Phi(\alpha_j + x_i^\top \beta_j) > \epsilon\}$ and $c_i^{(\epsilon)} = \sum_{j=1}^p c_{ij}^{(\epsilon)}$ denote the number of common species with threshold ϵ for sample i ($i = 1, \dots, n$). For TRACE, the expected number of common species

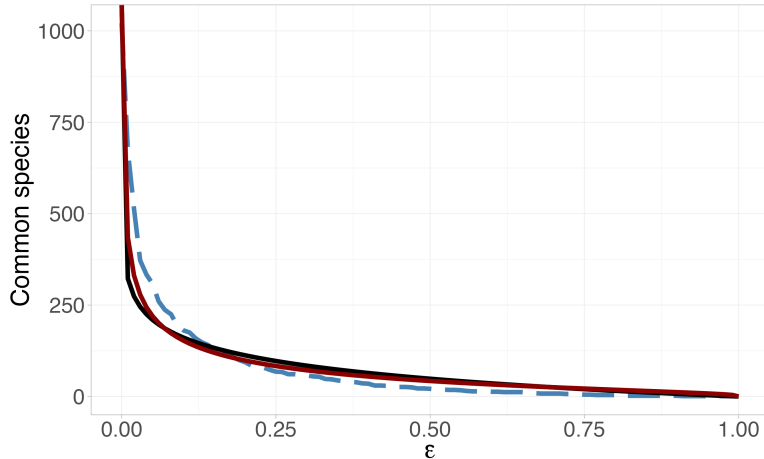


Figure 2: Expected total number of common species for the **TRACE** (red line) and **IBP** (black line) models for different values of ϵ , with $\gamma = 70$. The dashed blue line shows the empirical number of common species for a grid of values of ϵ for the fungi co-occurrence data.

for sample i is

$$\lim_{p \rightarrow \infty} E(c_i^{(\epsilon)}) = \gamma \exp \left\{ -\Phi^{-1}(\epsilon) + x_i^\top \nu + (1/2)x_i^\top \Psi x_i - 0.5 \right\} = \gamma g_i \exp \{ -\Phi^{-1}(\epsilon) - 0.5 \}.$$

As in Theorem 2 for the expected sample-specific species richness, we obtain a quadratic regression model for the log of the expected number of common species. Remarkably, the expected number of common species in a sample is simply the expected sample-specific species richness multiplied by $\exp\{-\Phi^{-1}(\epsilon) - 0.5\}$.

In biodiversity studies, the total number of species observed in a study, or overall species richness, is of key interest. This quantity corresponds to the number of non-zero columns of Y observed in n samples, which we denote as p_n^* . Griffiths and Ghahramani (2011) showed that the expected value of p_n^* for the **IBP** is γH_n , where H_n is the n th harmonic number, and thus the number of nonzero columns grows as $\mathcal{O}(\gamma \log n)$. Theorem 3 shows that the growth rate for the no covariates **TRACE** model is the same, while providing further insights into the expected value and distribution of p_n^* in the simple case with $\Sigma = I$.

Theorem 3. Consider the no covariates **TRACE** model and let $w_j = \mathbb{1}(n_j > 0)$ and $p_n^* = \sum_{j=1}^p w_j$. Then for $p \rightarrow \infty$ (i) p_n^* grows as $\mathcal{O}(\gamma \log n)$; (ii) $\gamma(H_n - a) < E(p_n^*) < \gamma(H_n - b)$, with $a = 0.073$ and $b = 0.02$. If we further assume $\Sigma = I$, then $p_n^* \sim \text{Poisson}(l)$ with $(H_n - a) < l < (H_n - b)$ for $p \rightarrow \infty$.

2.3 CORRELATION STRUCTURE AND PRIOR ELICITATION

The **TRACE** model defined in (2) and (3) provides a general framework that can be used in different settings under appropriate choices of the correlation matrix. Here, we propose alternative approaches to

model Σ for reducing dimensionality and overcoming the inferential challenges of rare species. Defining a structure that induces shrinkage in the correlation matrix is essential, considering the limited data available for accurately estimating its elements.

We consider two different models for the correlation matrix Σ . The first assumes a common correlation coefficient for all pairs of species, $\rho_{jj'} = \rho$. We induce a prior for ρ by letting the corresponding Fisher transformation $\zeta = 0.5 \log\{(1 + \rho)/(1 - \rho)\}$ with $\zeta \sim N(0, w_0^2)$. Besides being a simple dependence structure, this formulation effectively reduces the dimensionality of Σ and may be realistic in certain contexts. For instance, a common positive correlation can be induced by including a random intercept $\xi_i \sim N(0, \lambda)$ in (2) measuring how beneficial the conditions are in general to all the different species under study.

As a more flexible alternative, we also consider a hierarchical model that lets

$$\zeta_{jj'} = 0.5 \log\{(1 + \sigma_{jj'})/(1 - \sigma_{jj'})\} \sim N(0, \omega^2), \quad \omega^2 \sim IG(a_\omega, b_\omega), \quad (6)$$

where $IG(a, b)$ is an inverse-gamma distribution. This hierarchical model shrinks the correlation coefficients towards a common mean; such shrinkage is particularly important for rare species. Correlation matrices sampled from (6) that fall outside the positive definite cone can be discarded. We find in practice that checking whether Σ is positive definite adds significantly to the computational burden when p is very large without improving practice performance in conducting inferences based on marginal posterior distributions for B and $\sigma_{jj'}$, which is the primary focus in applications. We will show empirically that this approach has improved performance relative to using the popular LKJ prior (Lewandowski et al., 2009).

This hierarchical prior structure can be easily integrated into the algorithm for posterior inference that we will present in the next section. To complete a Bayesian specification of the TRACE model, we choose a gamma prior for the parameter γ , $\gamma \sim Ga(a_\gamma, b_\gamma)$.

2.4 POSTERIOR COMPUTATION

Posterior inference is conducted by truncating the number of species at a suitably large value p , which is substantially greater than the observed number of species p_n^* . Truncation is standard practice in nonparametric Bayesian models involving infinitely-many components, ranging from mixture models (Ishwaran and James, 2001) to latent feature models (Williamson et al., 2010; Doshi et al., 2009). In the supplementary materials, we provide simulation results showing that posterior inferences for the TRACE model are robust with respect to the choice of truncation level.

Fitting TRACE presents the key computational challenge of evaluating multivariate Gaussian orthant probabilities. A common strategy in fitting multivariate probit models is the use of data augmentation with latent variables simulated from truncated multivariate Gaussian distributions (Chib and

Greenberg, 1998). However, this approach is impractical for **TRACE**. Sampling from high dimensional truncated Gaussian distributions is computationally prohibitive and remains an active research area. Additionally, for imbalanced binary data, Johndrow et al. (2019) showed that Markov chain Monte Carlo algorithms relying on data augmentation suffer from poor mixing. Large numbers of rare species results in a highly imbalanced setting, making the mixing issue particularly problematic.

To facilitate scaling to large numbers of species, one possibility is to adapt a recently proposed algorithm for rapid posterior computation in multivariate probit models (Chakraborty et al., 2023). This algorithm focuses on approximating marginal posterior distributions for the parameters, obtaining accurate point estimation and uncertainty quantification. It is built on a Laplace approximation strategy (Tierney and Kadane, 1986). The detailed steps of the algorithm for posterior inference for **TRACE** are given in Section S.2 of the supplementary materials.

3 PERFORMANCE ASSESSMENTS IN SIMULATIONS

We evaluate the performance of **TRACE** through simulation studies. One performance metric is estimation accuracy relative to the true marginal occurrence probabilities $\pi_{ij}^* = \Phi(\alpha_j^* + x_i^\top \beta_j^*)$ and true correlation matrix Σ^* . In addition, in ecological applications there is substantial interest in predicting the number of new species that would be discovered if m additional samples were collected; we assess the performance of such predictions. The focus is to predict conditionally on p_n^* the number of new species discovered in an additional m samples, $\Delta_{m|n} = p_{n+m}^* - p_n^*$. We will focus on predicting the number of new species in the last 20 samples, with the key quantity being $\Delta_{100|80}^* = p_{100}^* - p_{80}^*$.

We compare with the **IBP** and a multivariate probit model with data matrix augmented with zeros for all columns j such that $p_n^* < j \leq p$. Inference in the **IBP** model proceeds through a Gibbs sampler, considering a gamma prior for γ and following the truncated beta-binomial representation of Griffiths and Ghahramani (2011). For the **IBP** and **TRACE** models, we set the parameters for the gamma prior on γ such that the distribution is centered on the empirical mean of the number of species per sample. For **TRACE** we use either the hierarchical prior on Σ in (6) or the LKJ prior; results for the LKJ prior were significantly worse as shown in Figure S2 of the supplementary material. The multivariate probit model is estimated using the **bigMVP** R package, which implements the fast posterior algorithm discussed in Chakraborty et al. (2023), assuming a hierarchical normal prior on the regression coefficients and prior (6) for the correlation matrix.

To simulate the data we consider a fixed sample size of $n = 100$ and $q = 5$ covariates and vary the number of observed species p_n^* , which is upper bounded by $p = 500$. The parameter γ is varied, ranging from 1 to 20, obtaining 20 different simulated datasets. The different values of γ lead to different numbers of observed species, as outlined in Section 2.2; so with a constant sample size, a higher γ results in a larger number of species sampled. For each value of γ , we consider three data-

generating scenarios: 1) (factor) the data are simulated under the **TRACE** model in (2) and (3) with $\Sigma^* = \Lambda\Lambda^\top + I$ where Λ is a $p \times H$ matrix with $H = 50$ and $\lambda_{jh} \sim N(0, 1)$ 2) (tobit) the data are generated under a misspecified **TRACE** model where the underlying continuous data z_{ij} are generated as $z_i \sim t_{10}(\alpha^* + x_i^\top B^*, \Sigma^*)$, where $t_{10}(\mu, \Sigma)$ denotes a multivariate t distribution with 10 degrees of freedom with mean μ and scale matrix Σ and have the same correlation structure as above and 3) (common) the data are simulated under the **TRACE** model where $\Sigma^* = \rho 1_p 1_p^\top + (1 - \rho)I$ with 1_p a p -dimensional vector of all ones and ρ drawn from a uniform distribution in $(0, 0.8)$. The latter scenario includes cases where $\Sigma = I$ or has a very similar formulation, resembling the Indian buffet process model construction. Elements of the design matrix are simulated from $N(0, 1)$ and the regression coefficients β_{jl}^* are drawn from $N(0, 1)$. We also simulate synthetic data in the three scenarios described above removing the covariates.

We compare the methods via estimation errors of π_j^* , $\Delta_{100|80}^*$ and Σ^* using $\|\hat{\pi} - \pi^*\|/(nP)$ and $\|\hat{\Sigma} - \Sigma^*\|/p^2$ for any estimator $\hat{\pi}$ and $\hat{\Sigma}$, where $\|\cdot\|$ is the Frobenius norm. In the setting without covariates, the error for the marginal occurrence probabilities is defined in terms of the vector L2 norm. For all methods we consider as estimators the posterior means. By observing that in IBP-type models with independent rows $E(p_n^*) = \sum_{j=1}^p w_j$ with $w_j \sim \text{Bernoulli}\{1 - (1 - \pi_j)^n\}$, it follows that $E(p_n^*) = \sum_{j=1}^p \{1 - (1 - \pi_j)^n\}$. From the latter, the expected value of $\Delta_{m|n}^*$ can be derived immediately. In the regression setting dependence among species led to a more complex expression, so we obtain an estimator of $\Delta_{m|n}^*$ by simulating from the posterior distribution. We compute mean square errors for each estimator $\hat{\Delta}_{100|80}$, using posterior means for all methods.

Figure 3 shows the results for the 20 simulations in each scenario for the **TRACE**, **IBP** and multivariate probit models. The top panel shows the results for the no covariates models, while the bottom panel is for the regression framework. Across all scenarios, the **TRACE** model consistently performs better or obtains comparable performance to the best competitor in terms of all three performance metrics. The multivariate probit model performs poorly in estimating $\Delta_{100|80}^*$, as it does not allow a growing number of outcomes, making it inadequate for predicting the number of new species in additional samples. The **IBP** model performs worst in estimating the correlation matrix since it assumes a fixed identity matrix. Additionally, its performance in estimating marginal occurrence probabilities is poor in the regression setting, as it fails to incorporate covariate dependence. Figure S3 of the supplementary materials shows that the results for **TRACE** are robust to changes in the truncation level.

4 FUNGAL BIODIVERSITY APPLICATION

We analyze data from a fungi biodiversity study in Finland (Abrego et al., 2018). Fungi are a highly diverse group of organisms, they play major roles in ecosystem functioning and are important for human health, food production and nature conservation. Data consist of 134 samples from different

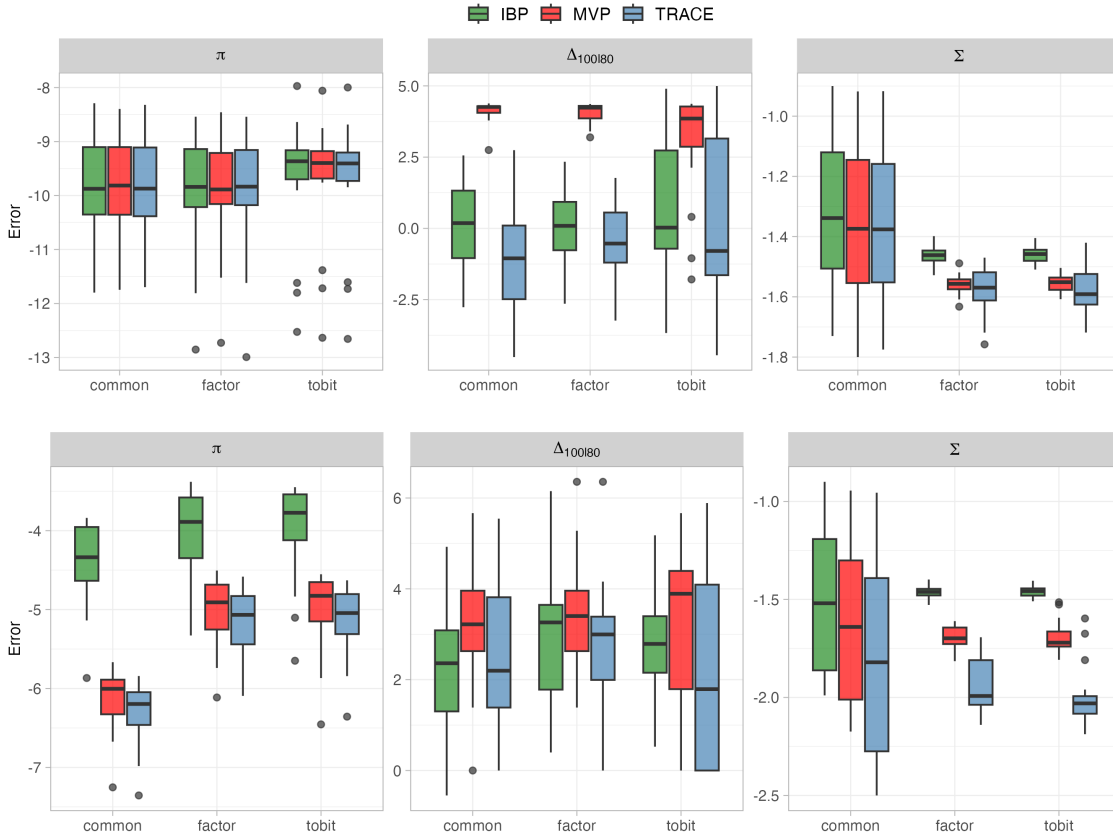


Figure 3: Logarithm of Frobenius errors for π^* , Σ^* and $\Delta_{100|80}^*$ of the TRACE (blue), IBP (green) and multivariate probit (red) models in 20 simulations for each scenario for no covariates settings (top-panel) and regression settings (bottom panel).

sites across four study locations in Finland, with 29 samples in Site 1, 97 samples in Site 2, 2 samples in Site 3 and 6 samples in Site 4. A cyclone sampler was used to acquire spore samples from each study site. Based on a probabilistic molecular species classifier using DNA barcoding, 1021 distinct species were identified. For each sample, the data include two covariates: a categorical variable with four levels indicating the study location and a continuous variable that provides information about the week. To assess any temporal dependence or effect of habitat type, we include these covariates in the model as predictors. We encode the site variable through three dummies with Site 2, having the highest number of observations, as the reference.

Given the massive number of fungal species identified and the presence of many rare species, we analyze the data with the hierarchical formulation for the correlation matrix of the TRACE model described in Section 2.3. This approach enables information sharing among species and achieves computational efficiency. Similarly to the simulations, we center the distribution of γ on the empirical mean of the number of species per sample. For the regression coefficients we use a normal prior centered

on zero, $\beta_j \sim N_q(0, \psi I)$. This choice led to a better fit to the data with respect to the hierarchical formulation for the regression coefficients defined in (4), and is less computationally demanding. Code to implement TRACE and replicate our analysis is available at <https://github.com/federicastolf/TRACE>.

To illustrate the taxonomical fungal composition in the study, we constructed Krona wheels (Ondov et al., 2011), which show the taxonomic composition of the operational taxonomic units (OTUs) found and their relative abundance. As a measure of relative species abundance, we used the posterior mean of the marginal occurrence probabilities of each species. The results are shown in Figure 4. Polyporales and Agaricales are the dominating Basidiomycota orders, whereas Helotiales and Lecanorales are the dominating Ascomycota orders. For an interactive version of the Krona wheel, allowing a detailed examination of each taxonomic level and showcasing changes as covariate values vary, see supplementary materials. It is interesting to see how these marginal occurrence probabilities change with location-specific covariates. For instance, the proportion of Ascomycota and Basidiomycota remains similar across three sites, but it differs for Site 4, where fewer Ascomycota species are present. This distinction may be linked to the specific characteristics of Site 4, a small and highly isolated island devoid of trees, setting it apart from the other sites, which are characterized by expansive natural spruce-dominated forests (Abrego et al., 2018). The four locations across Finland exhibit significant differences in sample-specific species richness, as illustrated in Figure S5 of the supplementary material. Specifically, Site 1 shows greater species richness than other sites, consistent with the findings in Abrego et al. (2018).

The matrix Σ captures dependence in co-occurrence, which is of interest in studying species interactions. Considering the correlation coefficients different from zero based on 90% credible intervals, the correlation matrix exhibits a sparse structure. While it is difficult to interpret the results on the species level due to the large dimensionality, we can obtain interesting conclusions by grouping species that fall in the same branch of the taxonomic tree; for example, species of the same order. As illustration, we focus on order pairs exhibiting the highest relative frequency of correlations different from zero. Relative frequency refers to the total positive (or negative) correlations between two orders among all possible pairs of these two orders. We notice that different orders of lichenized fungi (Lücking et al., 2017) exhibit a positive correlation. In terms of positive relative frequency, the 33% of (Lecideales, Pertusariales) and (Umbilicariales, Phaeomoniellales), the 25% of (Lecideales, Baeomycetales), and the 23% of (Xylariales, Lecideales) are correlated in occurrence. Perhaps, environmental conditions that support one type of lichen are also favorable for other types. Another important group is mycorrhizal fungi, which are in symbiotic relationships with plant roots. We notice a positive correlation (50% in terms of positive relative frequency) between the Sebaciniales and Cantharellales orders of mycorrhizal fungi, likely due to the fact that both orders tend to form relationships with similar plant species such

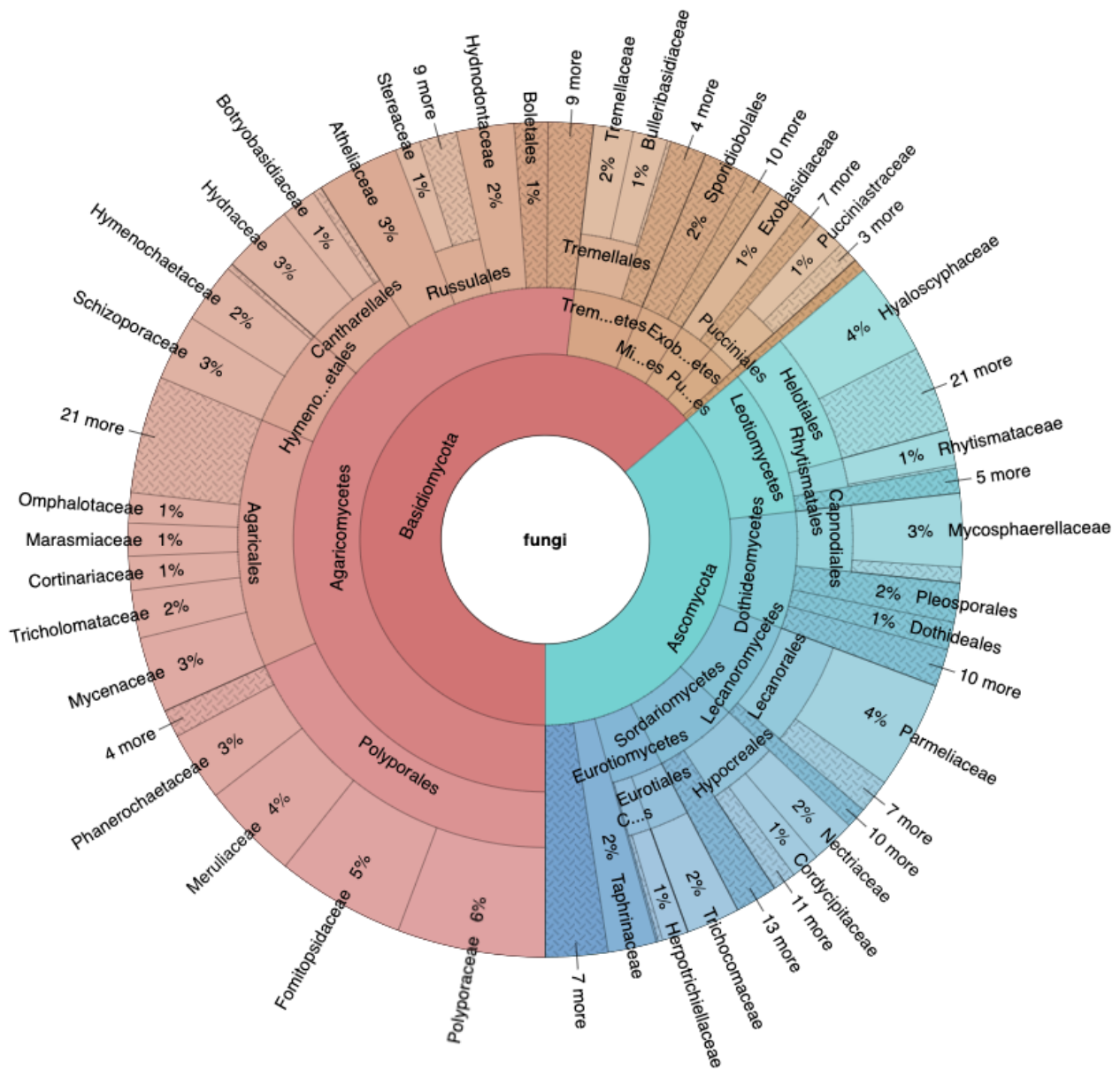


Figure 4: Fungal taxonomic composition and marginal species occurrence probabilities.

as orchids (Qin et al., 2020) which are widespread in Finland.

In biodiversity research, it is important to measure species richness, corresponding to the number of species in a community (Colwell, 2009). A commonly employed methodology for this purpose involves constructing species accumulation curves. These curves record the cumulative number of species found in an area as a function of the cumulative sampling effort. Initially, the curves exhibit a steep ascent as more samples are collected, but after the initial stages the curves are expected to exhibit a slower growth pattern, indicative of the inclusion of increasingly rare species. For a Bayesian nonparametric method that directly specifies a model for the accumulation curve see Zito et al. (2023).

Table 1: Performance of the **TRACE**, multivariate probit (MVP) and Indian buffet process (IBP) models in predicting discovery of new species of fungi in Finland for Site 1 and Site 2. The mean square error (MSE) is in logarithm scale.

	Site 1			Site 2		
	TRACE	IBP	MVP	TRACE	IBP	MVP
MSE p_n^* (median)	4.75	8.78	7.86	5.81	8.19	7.50
MSE p_n^* (IQR)	0.09	0.04	0.14	0.99	0.72	0.61

With this motivation, we estimate the sample species richness p_n^* under our model for Site 1 and Site 2, as the other sites have few samples. For Site 1, we randomly select a test set containing 25% of the observations and fit the **TRACE** model excluding these observations. Then, we draw 100 samples from the posterior predictive distributions of Y and count the cumulative total number of species across the different sample sizes, estimating p_n^* for each $n = 1, \dots, n_1$ with n_1 the total number of observations in the test set for Site 1. We compare to results from the same competitors of Section 3. For the **IBP**, we consider the same test set, but only use observations from Site 1 in training. To evaluate the models, we compute for each n ($n = 1, \dots, n_1$) a predictive mean square error for p_n^* . We followed the same procedure for Site 2. Table 1 shows, for the two sites, the median and the interquartile range of the above mean square errors computed from the different points in the test sets. The **TRACE** model consistently outperforms the competitors in predicting p_n^* for both sites.

5 DISCUSSION

In this article we propose a novel class of models for inference on multivariate binary outcomes having a growing dimension. While the developments were concretely motivated by biodiversity studies, the modeling framework has much broader applicability. The **TRACE** class maintains many of the desirable properties of the popular **IBP**, while addressing important statistical complexities that arise in applications, such as dependence in species occurrence, covariate effects and the need to borrow information in conducting inferences for rare species.

In introducing a class of **IBP**-type models that allow a flexible dependence structure across species, we are faced with a challenge of how to effectively characterize an increasing-dimensional correlation matrix. In fixed dimensional settings, it is common to rely on latent factor models to reduce dimensionality in characterizing dependence in multivariate binary data. However, such approaches cannot be directly applied in the **IBP** setting, which inevitably involves extremely sparse binary data and requires a coherent framework for prediction. For addressing this problem, we propose a hierarchical approach which effectively induces shrinkage in the modeling of the correlation matrix. This initial direction should motivate more work in this area; for example, alternative factor modeling approaches (perhaps related to Beraha and Griffin (2023)) or stochastic block model formulations that infer latent

communities of species based on their correlation structure.

There are many interesting directions for future research motivated directly by biodiversity studies. Firstly, most current IBP models impose a restrictive rate of discovery of new species as additional samples are taken. However, in exploratory data analyses, we found that fitting the empirical species accumulation curves from real world biodiversity studies often requires more flexibility. One promising direction in this regard is to introduce dependence in more sophisticated versions of the IBP, such as the three-parameter generalization with power-law behaviour of Teh and Gorur (2009).

Another important direction is making our statistical tools sufficiently computationally efficient and off-the-shelf so that ecologists can use them routinely. Joint species distribution models have become routinely used in ecology, but their inference methods cannot handle new species discovery and/or the presence of many rare species in the sample. It is of substantial importance to be able to predict future species discovery based on current samples, while accurately characterizing uncertainty and accommodating effects of climate change and other covariates. It is additionally of substantial interest to infer which species are endangered and should be added to so-called red lists. Our statistical tools provide a first step towards automating such inferences and decisions.

ACKNOWLEDGEMENT

This project has received funding from the European Research Council under the European Union’s Horizon 2020 research and innovation programme (grant agreement No 856506).

REFERENCES

- Abramowitz, M. and I. A. Stegun (1948). *Handbook of Mathematical Functions with Formulas, Graphs, and Mathematical Tables*, Volume 55. US Government Printing Office.
- Abrego, N., B. Furneaux, B. Hardwick, P. Somervuo, I. Palorinne, C. A. Aguilar-Trigueros, N. R. Andrew, U. V. Babiy, T. Bao, G. Bazzano, et al. (2024). Airborne DNA reveals predictable spatial and seasonal dynamics of fungi. *Nature* *631*, 835–842.
- Abrego, N., V. Norros, P. Halme, P. Somervuo, H. Ali-Kovero, and O. Ovaskainen (2018). Give me a sample of air and I will tell which species are found from your region: Molecular identification of fungi from airborne spore samples. *Mol. Ecol. Res.* *18*(3), 511–524.
- Beraha, M. and J. E. Griffin (2023). Normalised latent measure factor models. *J. R. Statist. Soc. B* *85*(4), 1247–1270.

- Broderick, T., J. Pitman, and M. I. Jordan (2013). Feature allocations, probability functions, and paintboxes. *Bayesian Anal.* 8, 801–836.
- Camerlenghi, F., S. Favaro, L. Masoero, and T. Broderick (2024). Scaled process priors for Bayesian nonparametric estimation of the unseen genetic variation. *J. Am. Statist. Assoc.* 119(545), 320–331.
- Chakraborty, A., R. Ou, and D. B. Dunson (2023). Bayesian inference on high-dimensional multivariate binary responses. *J. Am. Statist. Assoc.* 0(0), 1–12.
- Chib, S. and E. Greenberg (1998). Analysis of multivariate probit models. *Biometrika* 85(2), 347–361.
- Colwell, R. K. (2009). Biodiversity: concepts, patterns, and measurement. *The Princeton Guide to Ecology* 663, 257–263.
- Di Benedetto, G., F. Caron, and Y. W. Teh (2020). Non-exchangeable feature allocation models with sublinear growth of the feature sizes. In *Proc. Int. Conf. Artif. Intel. Statist.*, Volume 108, pp. 3208–3218. PMLR.
- Doshi, F., K. Miller, J. Van Gael, and Y. W. Teh (2009). Variational inference for the Indian buffet process. In *Proc. 12th Int. Conf. Artif. Intel. Statist.*, Volume 5, pp. 137–144. PMLR.
- Drezner, Z. and G. O. Wesolowsky (1990). On the computation of the bivariate normal integral. *J. Statist. Comput. Simul.* 35(1-2), 101–107.
- Genz, A. (1992). Numerical computation of multivariate normal probabilities. *J. Comput. Graphic. Statist.* 1(2), 141–149.
- Gershman, S. J., P. I. Frazier, and D. M. Blei (2014). Distance dependent infinite latent feature models. *IEEE Trans. Neural Networks Learn. Syst.* 37(2), 334–345.
- Griffiths, T. and Z. Ghahramani (2011). The Indian buffet process: An introduction and review. *J. Mach. Learn. Res.* 12(32), 1185–1224.
- Ishwaran, H. and L. F. James (2001). Gibbs sampling methods for stick-breaking priors. *J. Am. Statist. Assoc.* 96(453), 161–173.
- Johndrow, J. E., A. Smith, N. Pillai, and D. B. Dunson (2019). Mcmc for imbalanced categorical data. *J. Am. Statist. Assoc.* 114(527), 1394–1403.
- Lee, S., J. Z. Huang, and J. Hu (2010). Sparse logistic principal components analysis for binary data. *Ann. Appl. Statist.* 4(3), 1579.
- Lewandowski, D., D. Kurowicka, and H. Joe (2009). Generating random correlation matrices based on vines and extended onion method. *J. Multiv. Anal.* 100(9), 1989–2001.

- Lücking, R., B. P. Hodkinson, and S. D. Leavitt (2017). The 2016 classification of lichenized fungi in the Ascomycota and Basidiomycota - Approaching one thousand genera. *The Bryologist* 119(4), 361–416.
- Ondov, B. D., N. H. Bergman, and A. M. Phillippy (2011). Interactive metagenomic visualization in a Web browser. *BMC Bioinform.* 12(385), 1–10.
- Ovaskainen, O., N. Abrego, P. Halme, and D. B. Dunson (2016). Using latent variable models to identify large networks of species-to-species associations at different spatial scales. *Meth. Ecol. Evol.* 7(5), 549–555.
- Owen, D. B. (1980). A table of normal integrals. *Communic. Statist. Simul. Comput.* 9(4), 389–419.
- Qin, J., W. Zhang, S.-B. Zhang, and J.-H. Wang (2020). Similar mycorrhizal fungal communities associated with epiphytic and lithophytic orchids of *Coelogyne corymbosa*. *Plant Diversity* 42(5), 362–369.
- Somervuo, P., S. Koskela, J. Pennanen, R. Henrik Nilsson, and O. Ovaskainen (2016). Unbiased probabilistic taxonomic classification for DNA barcoding. *Bioinformatics* 32(19), 2920–2927.
- Teh, Y. and D. Gorur (2009). Indian buffet processes with power-law behavior. In *Advanc. Neur. Inform. Process. Syst.*, Volume 22. Curran Associates, Inc.
- Thibaux, R. and M. I. Jordan (2007). Hierarchical beta processes and the Indian buffet process. In *Proc. 11th Int. Conf. Artif. Intel. Statist.*, Volume 2, pp. 564–571. PMLR.
- Tierney, L. and J. B. Kadane (1986). Accurate approximations for posterior moments and marginal densities. *J. Am. Statist. Assoc.* 81(393), 82–86.
- Tikhonov, G., O. H. Opedal, N. Abrego, A. Lehtikoinen, M. M. J. de Jonge, J. Oksanen, and O. Ovaskainen (2020). Joint species distribution modelling with the r-package HMSC. *Meth. Ecol. Evol.* 11(3), 442–447.
- Warr, R. L., D. B. Dahl, J. M. Meyer, and A. Lui (2022). The attraction Indian buffet distribution. *Bayesian Anal.* 17(3), 931–967.
- Williamson, S., P. Orbanz, and Z. Ghahramani (2010). Dependent Indian buffet processes. In *Proc. 13th Int. Conf. Artif. Intel. Statist.*, Volume 9, pp. 924–931. PMLR.
- Zhao, X., G. Plata, and P. D. Dixit (2021). SiGMoiD: A super-statistical generative model for binary data. *PLoS Comput. Biol.* 17(8), e1009275.
- Zito, A., T. Rigon, O. Ovaskainen, and D. B. Dunson (2023). Bayesian modeling of sequential discoveries. *J. Am. Statist. Assoc.* 118(544), 2521–2532.

SUPPLEMENTARY MATERIALS

S.1 PROOFS

S.1.1 PROOF OF THEOREM 1

We start by computing the $p \rightarrow \infty$ limit of the expected value of $n_i = \sum_{j=1}^p y_{ij}$ for the no covariates TRACE. Let $\phi(\cdot)$ denote the density function of a standard normal variable. The expected value of the number of species per sample n_i for each $i = 1, \dots, n$ is

$$E(n_i) = \sum_{j=1}^p \int_{-\infty}^{\infty} \Phi(\alpha_j) \frac{1}{\tau_p} \phi\left(\frac{\alpha_j - \mu_p}{\tau_p}\right) d\alpha_j = \sum_{j=1}^p \int_{-\infty}^{\infty} \Phi(\tau_p \alpha_j + \mu_p) \phi(\alpha_j) d\alpha_j. \quad (7)$$

Owen (1980) showed that (7) is equal to $\sum_{j=1}^p \Phi\{\mu_p/(1 + \tau_p^2)^{1/2}\}$. Then, by substituting μ_p in the latter expression we obtain

$$E(n_i) = p \frac{\gamma/p}{\gamma/p + 1},$$

that converges to γ as $p \rightarrow \infty$ for each $i = 1, \dots, n$.

If we further assume $\Sigma = I$, then n_i is a sum of independent Bernoulli random variables and thus it is a binomial distribution with size p and success probability $(\gamma/p)/(\gamma/p + 1)$. Given that $p\{(\gamma/p)/(\gamma/p + 1)\}$ converges to γ for $p \rightarrow \infty$, it follows by the law of rare events that n_i converges to a Poisson distribution of parameter γ .

S.1.2 PROOF OF PROPOSITION 1

Recalling that the observations for different species are not independent, the variance of $n_i = \sum_{j=1}^p y_{ij}$ is $\text{var}(n_i) = \sum_{j=1}^p \text{var}(y_{ij}) + \sum_{j < j' \leq p} \text{cov}(y_{ij}, y_{ij'})$, where

$$\text{cov}(y_{ij}, y_{ij'}) = E(y_{ij}y_{ij'}) - \frac{p(p-1)}{2} \frac{\gamma^2}{(\gamma+p)^2},$$

and applying the law of total variance, the variance of the observations in the no covariates TRACE is

$$\text{var}(y_{ij}) = E[\Phi(\alpha_j)\{1 - \Phi(\alpha_j)\}] + \text{var}\{\Phi(\alpha_j)\} = E\{\Phi(\alpha_j)\} - E\{\Phi(\alpha_j)\}^2 = \frac{\gamma}{\gamma+p} - \frac{\gamma^2}{(\gamma+p)^2}.$$

From the last equation it easily follows that $\lim_{p \rightarrow \infty} \sum_{j=1}^p \text{var}(y_{ij}) = \gamma$. This is the variance of n_i if one assumes independence among species, so the covariance between y_{ij} and $y_{ij'}$ is zero. Thus, the limit for $p \rightarrow \infty$ of the variance of n_i is

$$\lim_{p \rightarrow \infty} \text{var}(n_i) = \gamma - \frac{\gamma^2}{2} + \lim_{p \rightarrow \infty} \sum_{j < j' \leq p} E(y_{ij}y_{ik}). \quad (8)$$

In the following we will focus on the more challenging part of obtaining an analytical expression for the $p \rightarrow \infty$ limit of $E(y_{ij}y_{ik})$, which involves a bivariate Gaussian orthant probability. The expected value of the product of y_{ij} and $y_{ij'}$ is equal to

$$E\{\Phi_2(\alpha; \sigma_{jj'})\} = \int_{-\infty}^{\infty} \int_{-\infty}^{\infty} \Phi_2(\alpha; \sigma_{jj'}) \frac{1}{\tau_p^2} \phi\left(\frac{\alpha_j - \mu_p}{\tau_p}\right) \phi\left(\frac{\alpha_{j'} - \mu_p}{\tau_p}\right) d\alpha_j d\alpha_{j'}, \quad (9)$$

where $\Phi_2(\alpha; \sigma_{jk})$ is the cumulative distribution function of a bivariate normal evaluated at $\alpha = (\alpha_j, \alpha_{j'})^\top$ with mean zero and correlation σ_{jk} . Drezner and Wesolowsky (1990) showed that the cumulative distribution function of a bivariate normal can be written as

$$\begin{aligned} \Phi_2(\alpha; \sigma_{jj'}) &= \Phi(\alpha_j)\Phi(\alpha_{j'}) + \frac{1}{2\pi}I(\sigma_{jj'}), \\ I(\sigma_{jj'}) &= \int_0^{\sigma_{jj'}} \frac{1}{(1-u^2)^{1/2}} \exp\left\{-\frac{1}{2(1-u^2)}(\alpha_j^2 - 2\alpha_j\alpha_{j'}u + \alpha_{j'}^2)\right\} du. \end{aligned}$$

Then, substituting the above expression for the bivariate cumulative distribution function and leveraging the same result on integrals of normal cumulative distribution function (Owen, 1980) used in the proof of Theorem 1, equation (9) becomes

$$E(y_{ij}y_{ij'}) = \frac{\gamma^2}{(\gamma+p)^2} + \frac{1}{2\pi} \int_{-\infty}^{\infty} \int_{-\infty}^{\infty} I(\sigma_{jj'}) \frac{1}{\tau_p} \phi\left(\frac{\alpha_j - \mu_p}{\tau_p}\right) \frac{1}{\tau_p} \phi\left(\frac{\alpha_{j'} - \mu_p}{\tau_p}\right) d\alpha_j d\alpha_{j'}.$$

The latter result implies that, as p grows, the variance of n_i in (8) becomes

$$\lim_{p \rightarrow \infty} \gamma + \sum_{j < j' \leq p} \frac{1}{2\pi} \int_{-\infty}^{\infty} \int_{-\infty}^{\infty} I(\sigma_{jj'}) \frac{1}{\tau_p} \phi\left(\frac{\alpha_j - \mu_p}{\tau_p}\right) \frac{1}{\tau_p} \phi\left(\frac{\alpha_{j'} - \mu_p}{\tau_p}\right) d\alpha_j d\alpha_{j'}. \quad (10)$$

By the dominated convergence theorem, we first compute the limit of the integrand in (10) and then do the integration. Let $a_p \simeq b_p$ indicate that $\lim_{p \rightarrow \infty} a_p/b_p = 1$, that is a_p and b_p have the same order. Exploiting the following asymptotic expansion (Abramowitz and Stegun, 1948) for the inverse of the cumulative distribution function of a normal distribution

$$\Phi^{-1}(x) \simeq -\{-2 \log x - \log(-2 \log x) - \log(2\pi)\}^{1/2} + o(1), \quad x \rightarrow 0,$$

we have $\mu_p \simeq -\{(1 + \tau_p^2)\{-2 \log\{\gamma/(\gamma+p)\} - \log[-2 \log\{\gamma/(\gamma+p)\}] - \log(2\pi)\}\}^{-1/2}$ for $p \rightarrow \infty$. Then, by standard convergence theorems we obtain the following equivalence

$$\lim_{p \rightarrow \infty} \frac{1}{\tau_p} \phi\left(\frac{\alpha_j - \mu_p}{\tau_p}\right) \frac{1}{\tau_p} \phi\left(\frac{\alpha_{j'} - \mu_p}{\tau_p}\right) = \lim_{p \rightarrow \infty} \exp\{-(1 + \alpha_j + \alpha_{j'})\} \frac{\gamma^2}{(\gamma+p)^2},$$

from which follows that the limit in (10) is equal to

$$\lim_{p \rightarrow \infty} \gamma + \exp(-1) \frac{\gamma^2}{(\gamma + p)^2} \sum_{j < j' \leq p} \frac{1}{2\pi} \int_{-\infty}^{\infty} \int_{-\infty}^{\infty} I(\sigma_{jj'}) \exp(-\alpha_j) \exp(-\alpha_{j'}) d\alpha_j d\alpha_{j'}.$$

Interchanging the order of integration with the Fubini-Tonelli theorem, the integrals in the latter expression become

$$\int_0^{\rho_{jj'}} \int_{-\infty}^{\infty} \int_{-\infty}^{\infty} \frac{1}{(1-u^2)^{1/2}} \exp \left\{ -\frac{\alpha_j^2 - 2\alpha_j \alpha_{j'} u + \alpha_{j'}^2}{2(1-u^2)} \right\} \exp(-\alpha_j - \alpha_{j'}) d\alpha_j d\alpha_{j'} du. \quad (11)$$

By completing the square for both α_j and $\alpha_{j'}$, we derive expressions that resemble the kernels of two normal densities and the subsequent integration with respect to both α_j and $\alpha_{j'}$ becomes straightforward. Then, by algebraic simplifications (11) can be expressed as $2\pi e \int_0^{\sigma_{jj'}} \exp(u) du = 2\pi \exp(1) |\exp(\sigma_{jj'}) - 1|$. We included the absolute value in the latter expression to consider both positive and negative correlations. Thus, as p grows the variance of n_i can be written as

$$\lim_{p \rightarrow \infty} \text{var}(n_i) = \gamma + \lim_{p \rightarrow \infty} \frac{\gamma^2}{(\gamma + p)^2} \sum_{j < j' \leq p} |\exp(\sigma_{jj'}) - 1|.$$

If we assume a finite number of correlation coefficients, $\sigma_{jj'} \in \{\rho_1, \dots, \rho_K\}$ with $K \in \mathbb{N}$, then $\sum_{j < j' \leq p} |\exp(\sigma_{jj'}) - 1| = \sum_{k=1}^K w_k |\exp(\rho_k) - 1|$, with $w_k = \sum_{j < j' \leq p} \mathbb{1}(\sigma_{jj'} = \rho_k)$ and $\sum_{k=1}^K w_k = p(p-1)/2$. Considering that $\sum_{k=1}^K w_k |\exp(\rho_k) - 1|$ is bounded above by $\{\max_k |\exp(\rho_k) - 1|\} p(p-1)/2$ and below by $\{\min_k |\exp(\rho_k) - 1|\} p(p-1)/2$, we conclude that

$$\gamma + \gamma^2/2 \{\min_k |\exp(\rho_k) - 1|\} \leq \lim_{p \rightarrow \infty} \text{var}(n_i) \leq \gamma + \gamma^2/2 \{\max_k |\exp(\rho_k) - 1|\}.$$

S.1.3 PROOF OF THEOREM 2

The expected value of the number of species per site i , $n_i = \sum_{j=1}^p y_{ij}$, for the TRACE model is

$$E(n_i) = \sum_{j=1}^p E(y_{ij}) = \sum_{j=1}^p \int_{-\infty}^{\infty} \Phi(u_{ij}) \frac{1}{(\tau_p^2 + x_i^\top \Psi x_i)^{1/2}} \phi \left\{ \frac{u_{ij} - x_i^\top \nu - \mu_p}{(\tau_p^2 + x_i^\top \Psi x_i)^{1/2}} \right\} du_{ij}, \quad (12)$$

with $u_{ij} = \alpha_j + x_i^\top \beta_j$ and following Owen (1980) we can show that (12) is equal to

$$\sum_{j=1}^p \Phi \left\{ \frac{\mu_p + x_i^\top \nu}{(1 + \tau_p^2 + x_i^\top \Psi x_i)^{1/2}} \right\}.$$

The $p \rightarrow \infty$ limit of the latter equation can be computed by leveraging the following asymptotic expansion (Abramowitz and Stegun, 1948) for the cumulative distribution function of a normal distribution

$$1 - \Phi(x) \simeq \frac{\exp(-x^2/2)}{(2\pi)^{1/2}x} + o\left(\frac{1}{x^2}\right), \quad x \rightarrow \infty.$$

Therefore, as p grows the expected value of n_i is

$$\lim_{p \rightarrow \infty} E(n_i) = \lim_{p \rightarrow \infty} \frac{p(\tau_p^2 + 1 + x_i^\top \Psi x_i)^{1/2}}{(2\pi)^{1/2}(-\mu_p - x_i^\top \nu)} \exp\left\{-\frac{(\mu_p + x_i^\top \nu)^2}{2(\tau_p^2 + 1 + x_i^\top \Psi x_i)^{1/2}}\right\}. \quad (13)$$

Employing the same asymptotic expansions for μ_p used in the proof of Proposition 1, the quantity $\exp[-(\mu_p + x_i^\top \nu)^2/\{2(\tau_p^2 + 1 + x_i^\top \Psi x_i)^{1/2}\}]$ as $p \rightarrow \infty$ is equivalent to

$$\exp\left\{\frac{2 \log(p)}{2 \log(p) + x_i^\top \Psi x_i + 1} \log\left(\frac{\gamma}{\gamma + p}\right)\right\} \left\{-2 \log\left(\frac{\gamma}{\gamma + p}\right)\right\}^{1/2} (2\pi)^{1/2} \exp(x_i^\top \nu - 1/2),$$

and analogously the quantity $(\tau_p^2 + 1 + x_i^\top \Psi x_i)^{1/2}/(-\mu_p - x_i^\top \nu)$ for $p \rightarrow \infty$ is equivalent to

$$\frac{\{1 + 2 \log(p) + x_i^\top \Psi x_i\}^{1/2}}{2 \log(p) - x_i^\top \nu}.$$

By further observing that by standard convergence theorems

$$\lim_{p \rightarrow \infty} \left\{-2 \log\left(\frac{\gamma}{\gamma + p}\right)\right\}^{1/2} \frac{\{1 + 2 \log(p) + x_i^\top \Psi x_i\}^{1/2}}{2 \log(p) - x_i^\top \nu} = 1,$$

it follows that the limit in (13) is equal to

$$\begin{aligned} \lim_{p \rightarrow \infty} E(n_i) &= \lim_{p \rightarrow \infty} p \exp(x_i^\top \nu - 1/2) \exp\left\{\frac{2 \log(p)}{2 \log(p) + x_i^\top \Psi x_i + 1} \log\left(\frac{\gamma}{\gamma + p}\right)\right\} \\ &= \gamma \exp\{1/2 + 0.5(x_i^\top \Psi x_i)\} \exp(x_i^\top \nu - 1/2) \\ &= \gamma \exp\{x_i^\top \nu + 0.5(x_i^\top \Psi x_i)\}, \end{aligned}$$

which concludes the proof of the first point of Theorem 2. The second point of Theorem 2 refers to the limiting variance of $n_i = \sum_{j=1}^p y_{ij}$, which is equal to

$$\lim_{p \rightarrow \infty} \text{var}(n_i) = \lim_{p \rightarrow \infty} p \text{var}(y_{ij}) + \frac{p(p-1)}{2} \text{cov}(y_{ij}, y_{ij'}).$$

By observing that $\lim_{p \rightarrow \infty} p E\{\Phi(\alpha_j + x_i^\top \beta_j)\} = \gamma g_i$ and $\lim_{p \rightarrow \infty} \{p(p-1)/2\} E\{\Phi(\alpha_j + x_i^\top \beta_j)\} = (\gamma g_i)^2/2$, with $g_i = \exp\{x_i^\top \nu + (1/2)x_i^\top \Psi x_i\}$, the above limit can be simply computed by adapting the same steps followed in the proof of Proposition 1.

S.1.4 PROOF OF PROPOSITION 3

The target is computing the $p \rightarrow \infty$ limit of the expected value of the number of common species for the no covariates TRACE model

$$E(c^{(\epsilon)}) = \sum_{j=1}^p \text{pr}\{\Phi(\alpha_j) > \epsilon\} = \sum_{j=1}^p \text{pr}\{\alpha_j > \Phi^{-1}(\epsilon)\} = p \left[1 - \Phi \left\{ \frac{\Phi^{-1}(\epsilon) - \mu_p}{\tau_p} \right\} \right].$$

Exploiting the same asymptotic expansion for the cumulative distribution function of a normal distribution used in the proof of Theorem 2, the limit of the expected value of $c^{(\epsilon)}$ is

$$\lim_{p \rightarrow \infty} E(c^{(\epsilon)}) = \lim_{p \rightarrow \infty} \frac{p\tau_p}{(2\pi)^{1/2}(\epsilon^* - \mu_p)} \exp \left\{ -\frac{1}{2\tau_p^2}(\epsilon^* - \mu_p)^2 \right\}, \quad (14)$$

with $\epsilon^* = \Phi^{-1}(\epsilon)$. Then, by leveraging the same asymptotic expansion for the inverse of the cumulative distribution function of a normal distribution used in the proof of Proposition 1 for μ_p , as $p \rightarrow \infty$ we obtain the following equivalences

$$\exp \left\{ -\frac{1}{2\tau_p^2}(\epsilon^* - \mu_p)^2 \right\} \simeq \exp(-\epsilon^*) \left(\frac{\gamma}{\gamma + p} \right) \left\{ -2 \log \left(\frac{\gamma}{\gamma + p} \right) \right\}^{1/2} (2\pi)^{1/2} \exp(-1/2),$$

$$\frac{\tau_p}{\epsilon^* - \mu_p} \simeq \frac{1}{[-2 \log\{\gamma/(\gamma + p)\}]^{1/2}}.$$

from which follows that the limit in (14) is equal to

$$\lim_{p \rightarrow \infty} E(c^{(\epsilon)}) = \lim_{p \rightarrow \infty} \exp \left(-\epsilon^* - \frac{1}{2} \right) p \left(\frac{\gamma}{\gamma + p} \right) = \gamma \exp \left(-\epsilon^* - \frac{1}{2} \right).$$

S.1.5 PROOF OF PROPOSITION 4

The expected value of the number of common species for sample i for the TRACE model is

$$E(c_i^\epsilon) = \sum_{j=1}^p \text{pr}\{\Phi(\alpha_j + x_i^\top \beta_j) > \epsilon\} = \sum_{j=1}^p \text{pr}\{\alpha_j + x_i^\top \beta_j > \Phi^{-1}(\epsilon)\},$$

and thus the goal is computing the following limit

$$\lim_{p \rightarrow \infty} p \left\{ 1 - \Phi \left(\frac{\Phi^{-1}(\epsilon) - \mu_p - x_i^\top \gamma}{(\tau_p + x_i^\top \Psi x_i)^{1/2}} \right) \right\},$$

that, leveraging the same asymptotic expansion for the inverse of the cumulative distribution function of a normal distribution used in the proof of Proposition 1 for μ_p , is equivalent to

$$\lim_{p \rightarrow \infty} \frac{p(\tau_p^2 + x_i^\top \Psi x_i)^{1/2}}{(2\pi)^{1/2}(\epsilon^* - \mu_p - x_i^\top \nu)} \exp \left\{ -\frac{(\epsilon^* - \mu_p - x_i^\top \nu)^2}{2(\tau_p^2 + x_i^\top \Psi x_i)^{1/2}} \right\},$$

with $\epsilon^* = \Phi^{-1}(\epsilon)$. The above equation is similar to equation (13) in the proof of Theorem 2. Hence, by simply adapting the same arguments discussed in the aforementioned proof we obtain

$$\lim_{p \rightarrow \infty} E(c_i^\epsilon) = \gamma \exp \left\{ -\epsilon^* + x_i^\top \nu + (1/2)x_i^\top \Psi x_i - 0.5 \right\}.$$

S.1.6 PROOF OF THEOREM 3

Let $w_j = \mathbf{1}(n_j > 0)$, with $n_j = \sum_{i=1}^n y_{ij}$, be binary random variables that indicate if column j is non empty. Then the number of non-empty columns is $p_n^* = \sum_{j=1}^p w_j$, where $w_j \sim Be\{1 - (1 - \pi_j)^n\}$ with $\pi_j = \Phi(\alpha_j)$ the marginal success probabilities. The aim is to compute $\lim_{p \rightarrow \infty} E(p_n^*) = \lim_{p \rightarrow \infty} \sum_{j=1}^p E\{1 - (1 - \pi_j)^n\}$. Exploiting binomial sum properties, one can write

$$(1 - \pi_j)^n = \sum_{k=0}^n \binom{n}{k} (-1)^k \pi_j^k,$$

from which follows that the limit as $p \rightarrow \infty$ of the expected value of p_n^* is equivalent to

$$\lim_{p \rightarrow \infty} \sum_{j=1}^p \left\{ -\sum_{k=1}^n \binom{n}{k} (-1)^k E(\pi_j^k) \right\}.$$

By leveraging Owen's integral table results (Owen, 1980), we can obtain a closed form for the moments of the marginal species occurrence probabilities π_j ,

$$E(\pi_j^k) = \int_{-\infty}^{\infty} \Phi(\alpha_j)^k \frac{1}{\tau_p} \phi\left(\frac{\alpha_j - \mu_p}{\tau_p}\right) d\alpha_j = \Phi_k(\mu_p \mathbf{1}_k; V_p),$$

where $V_p = I + \tau_p^2 \mathbf{1}_k^\top \mathbf{1}_k$ is a $k \times k$ covariance matrix and $\Phi_k(\mu_p \mathbf{1}_k; V_p)$ denotes the cumulative distribution function of the multivariate Gaussian $N_k(0_k, V_p)$ evaluated at $\mu \mathbf{1}_k$. Hence, the target quantity to compute, denoted as $L(p_n^*)$, becomes

$$L(p_n^*) = \lim_{p \rightarrow \infty} p \left\{ -\sum_{k=1}^n \binom{n}{k} (-1)^k \Phi_k(\mu_p \mathbf{1}_k; V_p) \right\}. \quad (15)$$

We first focus on computing $\lim_{p \rightarrow \infty} \Phi_k(\mu_p \mathbf{1}_k; V_p)$. Let $u = (u_1, \dots, u_k)^\top$ and recall that V_p^{-1} has diagonal elements equal to $\{\tau_p^2(k-1) + 1\}/(k\tau_p^2 + 1)$ and off-diagonal elements equal to $-\tau_p^2/(k\tau_p^2 + 1)$.

Then we have

$$\begin{aligned}
\Phi_k(\mu_p \mathbf{1}_k; V_p) &= \frac{|V_p|^{-1/2}}{(2\pi)^{k/2}} \int_{-\infty}^0 \cdots \int_{-\infty}^0 \exp \left\{ -\frac{1}{2} (u + \mu_p \mathbf{1}_k)^\top V_p^{-1} (u + \mu_p \mathbf{1}_k) \right\} du \\
&= \frac{(1 + k\tau_p^2)^{-1/2}}{(2\pi)^{k/2}} \exp \left(-\frac{1}{2} \mu_p^2 \mathbf{1}_k^\top V_p^{-1} \mathbf{1}_k \right) \int_{-\infty}^0 \cdots \int_{-\infty}^0 \exp \left(-\frac{1}{2} u V_p^{-1} u^\top - u V_p^{-1} \mu_p \mathbf{1}_k \right) du \\
&= \frac{(1 + k\tau_p^2)^{-1/2}}{(2\pi)^{k/2}} \exp \left(-\frac{1}{2} \frac{k\mu_p^2}{k\tau_p^2 + 1} \right) \int_{-\infty}^0 \cdots \int_{-\infty}^0 \exp \left(-\frac{1}{2} u V_p^{-1} u^\top - \frac{\mu_p}{k\tau_p^2 + 1} u \mathbf{1}_k \right) du.
\end{aligned}$$

Notice that as $p \rightarrow \infty$, the integral above, by standard convergence theorems, converges to

$$\int_{-\infty}^0 \cdots \int_{-\infty}^0 \exp \left\{ -\frac{1}{2} \sum_{i=1}^k u_i \left(\frac{k-1}{k} u_i + \frac{1}{k} \sum_{j \neq i} u_j \right) - \frac{1}{k} u^\top \mathbf{1}_k \right\} dx = C_k,$$

where C_k is a generic constant depending on k . Then, by using the same asymptotic expansion for $\Phi^{-1}\{\gamma/(\gamma+p)\}$ stated in the proof of Proposition 1, for $p \rightarrow \infty$ the following equivalence holds

$$\frac{(1 + k\tau_p^2)^{-1/2}}{(2\pi)^{k/2}} \exp \left(-\frac{1}{2} \frac{k\mu_p^2}{k\tau_p^2 + 1} \right) \simeq \frac{(1 + k2 \log p)^{-1/2} (2\pi)^{1/2}}{(2\pi)^{k/2} \exp(1/2)} \left(\frac{\gamma}{\gamma+p} \right) \left\{ -2 \log \left(\frac{\gamma}{\gamma+p} \right) \right\}^{1/2}.$$

From the latter equation it easily follows that $\Phi_k(\mu_p \mathbf{1}_k; V_p) \simeq \{\gamma/(\gamma+p)\} C_k$ for $p \rightarrow \infty$. Therefore, (15) is equal to

$$L(p_n^*) = \lim_{p \rightarrow \infty} p \left\{ -\sum_{k=1}^n \binom{n}{k} (-1)^k \left(\frac{\gamma}{\gamma+p} \right) C_k \right\} = \gamma \left\{ -\sum_{k=1}^n \binom{n}{k} (-1)^k C_k \right\},$$

which shows that the $p \rightarrow \infty$ limit of the expected value of p_n^* converges to a finite value.

Obtaining an expression for C_k involves integrating over a multivariate normal distribution and explicit formulas of orthant probability are only available for small values of k . However, leveraging the method proposed in Genz (1992) we can obtain a numerical evaluation of C_k . Recalling that the harmonic number can be written as $H_n = -\sum_{k=1}^n \binom{n}{k} (-1)^k (1/k)$, we have

$$L(p_n^*) = \gamma \left\{ H_n + \sum_{k=1}^n \binom{n}{k} (-1)^k d(k) \right\},$$

where $d(k) = C_k - 1/k$. The function $d(k)$ for $k \in (1, 1000)$ is a unimodal function; see Figure S1 for a graphical representation. We considered the function for $k \in (1, 1000)$ as this is a reasonable set of values for the sample size. For $k = 1$ the orthant probability has an analytical solution and $d(k) = 0$. Given that $\sum_{k=1}^n \binom{n}{k} (-1)^k = -1$, we can obtain the following bounds for the $p \rightarrow \infty$ limit of the

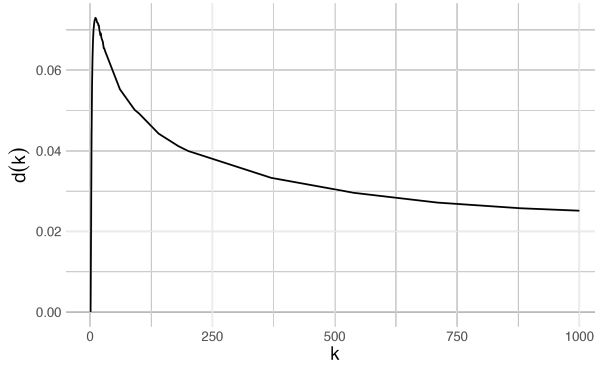


Figure S1: Graphical representation of the function $d(k)$.

expected value of p_n^*

$$\gamma(H_n - m_k) < L(p_n^*) < \gamma(H_n - u_k), \quad u_k = \max_{k \in (1, 1000)} d(k), \quad m_k = \min_{k \in (1, 1000)} d(k),$$

with $u_k = 0.02$ and $m_k = 0.073$. Therefore, considering that $H_n = \mathcal{O}(\log n)$, we can conclude that $L(p_n^*) = \mathcal{O}(\gamma \log n)$.

In the following part we will prove that, assuming independence among features, the number of non empty columns converges to a Poisson distribution as p grows. Assuming $\Sigma = I$ implies that p_n^* is a sum of independent Bernoulli random variables ω_j , and thus it is a binomial distribution with size p and success probability $c_p = -\sum_{k=1}^n \binom{n}{k} (-1)^k \left(\frac{\gamma}{\gamma+p}\right) C_k$. Given that pc_p converges to $l = \gamma\{-\sum_{k=1}^n \binom{n}{k} (-1)^k C_k\}$ for $p \rightarrow \infty$, it follows by the law of rare events that p_n^* converges to a Poisson distribution with parameter l .

S.2 POSTERIOR COMPUTATION

In this section we describe an algorithm for posterior inference under the **TRACE** model building on recent computational developments for multivariate probit models (Chakraborty et al., 2023). They develop a two-stage method based on Laplace approximations, which achieves optimal rates in estimating both regression parameters and correlation coefficients. For **TRACE** we focus on approximating marginal posterior distributions for the parameters, obtaining accurate point estimation, uncertainty quantification and predictions.

Let $b_j = (\alpha_j, \beta_j)^\top$ denote the random intercept α_j and regression coefficients β_j for species j . We first obtain approximations $\Pi_j^*(b_j | y)$ for the marginal posteriors of the random intercepts and regression coefficients for $j = 1, \dots, p$; we use a simplified likelihood that replaces Σ with the identity matrix and apply Laplace approximations. Let $l_j(b_j)$ denote the log-likelihood of the j th binary outcome under this simplified model and $\Pi_j(b_j)$ denote the prior distribution for b_j , with $\alpha_j \sim N(\mu_p, \tau_p^2)$,

$\beta_j \sim N_q(\nu, \Psi)$ and no correlation between the α_j s and the β_j s. Then $\Pi_j^*(b_j | y) \approx N(\hat{b}_j, Q_j)$, where $\hat{b}_j = \operatorname{argmax}_{b_j} \{l_j(b_j) + \log \Pi_j(b_j)\}$ and Q_j is the corresponding inverse Hessian. Chakraborty et al. (2023) showed in their Theorem 3.5 that $\Pi_j^*(b_j | y)$ is asymptotically normal centered at a maximum composite likelihood estimator with the appropriate variance.

We then proceed with obtaining approximations to the marginal posterior distributions of the elements of the correlation matrix Σ . We approximate the marginal posterior distributions of $\sigma_{jj'}$ by considering a bivariate probit model between the pairs (j, j') . We combine this likelihood with the marginal prior for $\sigma_{jj'}$ to obtain a Gaussian approximation $\Pi_{jj'}^*(\sigma_{jj'} | y)$ for the posterior of $\sigma_{jj'}$, as justified in Theorem 3.7 of Chakraborty et al. (2023). The mean $\hat{\sigma}_{jj'}$ and the variance $s_{jj'}^2$ of the approximate posteriors for $\sigma_{jj'}$ are obtained using Gauss-Legendre quadrature. Chakraborty et al. (2023) show that asymptotically the distribution is centered at the maximum composite likelihood estimator from the bivariate margins. In the common correlation matrix setting, assuming $\rho_{jj'} = \rho$, we use Metropolis-Hastings to sample from the conditional posterior of ρ given the b_j s; for this simple choice of correlation structure, we do not use the above asymptotic Gaussian approximation for the posterior of $\sigma_{jj'}$. Predictions can be obtained using pairwise approximations to the posterior predictive.

For the hierarchical formulation of the correlation matrix, where $\zeta_{jj'} \sim N(0, \omega^2)$, with $\sim IG(a_\omega, b_\omega)$, computations become more complex due to the additional dependence between $\sigma_{jj'}$ for different outcomes, induced through the shared ω . Nonetheless, we can adapt the previously described algorithm by conditioning on ω with minimal adjustments to account for the induced prior $\rho_{jj'}$. This allows us to create a fast approximate sampler by using empirical Bayes estimates of ω , a natural way to maintain computational scalability. A similar strategy can also be used to include a gamma prior on the TRACE parameters γ . Algorithm 1 summarizes the steps to obtain empirical Bayes estimation of γ and ω . In the common correlation coefficient case, the algorithm can be simplified as we do not need to estimate ω ; hence, we only repeat steps 1–3.

The same approach described in Algorithm 1 can be applied to incorporate the hierarchical prior on the regression coefficients, defined in equation (4) in the main paper. In this case, after have obtained an approximation of $\Pi(\beta_j | y, X, \nu, \Psi)$ with prior $\beta_j \sim N_q(\nu, \Psi)$ and having drawn a sample from the corresponding posterior of β_j , one can update (ν, Ψ) as $(\nu, \Psi) \sim \text{NIW}(\nu_p, \iota_p, d_p, \Xi_p)$, with $\iota_p = \iota + p$, $d_p = d + p$, $\nu_p = (\iota\nu_0 + p\hat{\beta})/\iota_p$ with $\hat{\beta} = (\sum_{j=1}^p \beta_j)/p$ and $\Xi_p = \Xi + S + (p\iota/\iota_p) \sum_{j=1}^p (\beta_j - \nu_0)(\beta_j - \nu_0)^\top$ with $S = \sum_{j=1}^p (\beta_j - \hat{\beta})(\beta_j - \hat{\beta})^\top$.

As an alternative to the above composite-likelihood and Laplace-based posterior approximations, we additionally ran a wide variety of experiments using data augmentation Markov chain Monte Carlo algorithms targeting the exact posterior distribution. Such algorithms were not competitive with the above approach in terms of computational time or estimation accuracy.

Algorithm 1: Two-stage approximate conditional sampler for the hierarchical TRACE.

Initialize ω and γ .

1. Given γ obtain approximation to $\Pi(\alpha_j | y, \gamma)$ as $N(\hat{\alpha}_j, Q_j)$ for $j = 1, \dots, p$ with the prior $\alpha_j \sim N(\mu_p, \tau_p)$.
2. Draw $\alpha_j \sim N(\hat{\alpha}_j, Q_j)$ independently for $j = 1, \dots, p$.
3. Update γ through a Metropolis–Hastings step.
4. Given ω , obtain approximations to $\Pi(\sigma_{jj'} | y, \omega)$ as $N(\hat{\sigma}_{jj'}, s_{jk}^2)$ for $j < j' = 1, \dots, p$ with pseudo-priors $\Pi_j^*(\alpha_j | y)\Pi_{j'}^*(\alpha_{j'} | y)$.
5. Draw $\sigma_{jj'} \sim N(\hat{\sigma}_{jj'}, s_{jk}^2)$ independently and set $\zeta_{jj'} = 0.5 \log\{(1 + \sigma_{jj'})/(1 - \sigma_{jj'})\}$ for $j < j' = 1, \dots, p$.
6. Update $\omega^2 \sim IG\left\{\frac{p(p-1)}{2} + a_\omega, \frac{1}{2} \sum_{j < j'} \zeta_{jj'}^2 + b_\omega\right\}$

Repeat steps 1-6 T times to obtain T samples of ω and γ .

S.3 ADDITIONAL SIMULATIONS

In this section, we report results from additional simulation experiments. We start by showing the improved performance for the TRACE model with the hierarchical prior for Σ defined in (6) of the main paper with respect to the popular LKJ prior (Lewandowski et al., 2009). We considered the same simulation settings described in Section 3 of the main paper and we set the LKJ parameter to one. Figure S2 shows the performance in estimating Σ^* for the TRACE model using either the hierarchical prior or the LKJ prior for the correlation matrix. While the accuracy in estimating π^* and $\Delta_{100|80}^*$ was comparable between the two models, the TRACE model with a hierarchical prior on the correlation matrix consistently outperformed the TRACE model with a LKJ prior in estimating the true correlation matrix across all scenarios. The results are consistent in the regression and the no covariates cases.

Subsequently, we provide simulation results demonstrating that posterior inference for the TRACE model is robust with respect to the choice of the truncation level for the number of species. We simulate 20 datasets with the same values for γ and n used in Section 3 of the main paper, and consider three different truncation levels for the number of species $p \in \{400, 500, 600\}$ for each of the 20 simulations. We assess the performance of TRACE in estimating Σ^* , π^* and $\Delta_{100|80}^*$ through the same metrics outlined in Section 3 of the main paper. For illustration purposes, we show the results for the ‘factor’ scenario with no covariates, but the performances were comparable across all scenarios and similar results were obtained for the covariate-dependent settings as well. The results, displayed in Figure S3, show that the error metrics for all quantities of interest maintain the same error order across the different truncation levels.

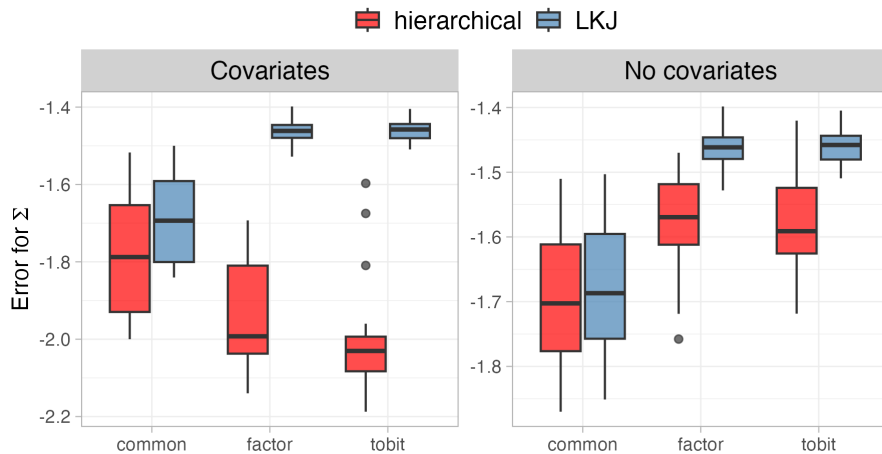


Figure S2: Logarithm of Frobenius errors for Σ^* for the TRACE model with LKJ and hierarchical priors for Σ in 20 simulations for each scenario in no covariates (left) and covariates (right) cases.

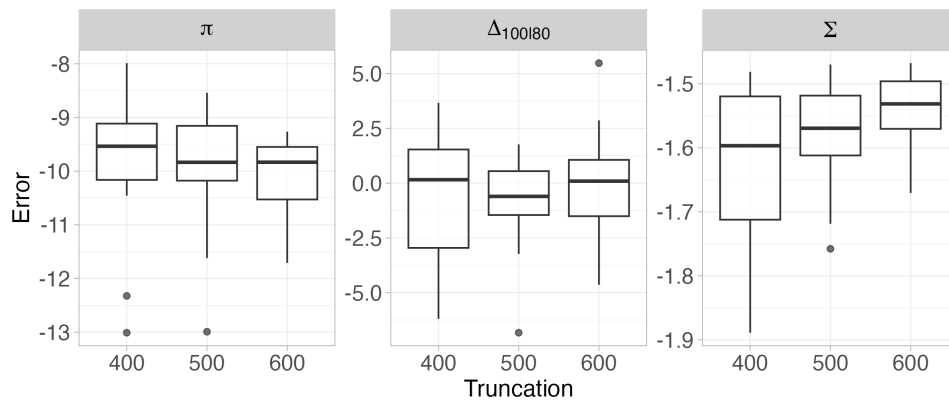


Figure S3: Logarithm of Frobenius errors for π^* , Σ^* and $\Delta_{100|80}^*$ of the TRACE model in 20 simulations for different truncation levels.

S.4 ADDITIONAL PLOTS FOR FUNGAL BIODIVERSITY APPLICATION

Figure S4 shows a snapshot of the Krona wheel plot specific to Site 3 and Site 4, highlighting the differences in fungal taxonomic composition among the different sites. As a measure of relative species abundance, we used the posterior mean of the marginal occurrence probabilities of each species. For an interactive version of the Krona wheel plots see <https://github.com/federicastolf/TRACE>.

Figure S5 shows the posterior means of sample-specific species richness across the four different locations in Finland over weeks. The week values cover the entire fruiting period, from early spring (week 0) to late autumn (week 22). Overall, Site 1, the one located in central Finland, exhibits greater species richness compared to the other ones. This site shows seasonal variation in community composition, with a decreasing trend in species richness over late spring and summer, as observed in

Abrego et al. (2018).



Figure S4: Fungal taxonomic composition and marginal species occurrence probabilities for Site 3 (left) and Site 4 (right).

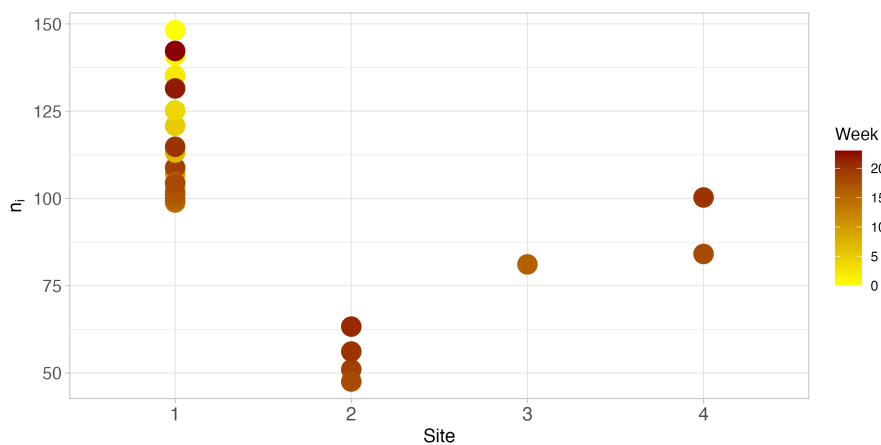


Figure S5: Posterior mean of sample-specific species richness for the four sites across weeks.